Poly(propylene-*co*-ethylene) Produced with a Conventional and a Self-Supported Ziegler–Natta Catalyst: Effect of Ethylene and Hydrogen Concentration on Activity and Polymer Structure

Torvald Vestberg,[1] Matthew Parkinson,[2] Isa Fonseca,[2] Carl-Eric Wilén[3]

[1]Borealis Polymers Oy, InnoTech PP catalyst, FIN-06101 Porvoo, Finland
[2]Borealis Polyolefine GmbH, InnoTech Operational Support, Linz 4021, Austria
[3]Functional Materials Center of Excellence, Laboratory of Polymer Technology,
Åbo Akademi University, FIN-20500 Åbo, Finland

ABSTRACT: A novel self-supported emulsion-based catalyst and a conventional $MgCl_2$-supported Ziegler–Natta catalyst were used in the copolymerization of propylene and ethylene under industrial conditions using triethyl aluminium as cocatalyst and dicyclopentyl dimethoxy silane as external donor. The effects of the concentration of ethylene and hydrogen on the polymerization behaviors and polymer properties were investigated. The combined effect of both ethylene and hydrogen increased the relative activity of the novel catalyst more than for the conventional catalyst. This trend was consistent with our earlier observed higher degree of dormancy, due to 2,1 insertions, found with the novel catalyst. More importantly, the work has uncovered that the self-supported catalyst incorporates ethylene in a more random fashion and produces copolymers with relatively narrow molecular weight distribution (MWD). These results in combination with polymer microstructure studies using Fourier transform infrared spectroscopy, ^{13}C-NMR spectroscopy, and differential scanning calorimetry all indicated that the novel catalyst has a narrower distribution of active site types than the conventional reference catalyst. The narrow composition of active site structures, the narrow MWD, and the random incorporation of ethylene into the polymer chain indicated that the emulsion-based catalyst possesses features that to a certain degree tend to be more indicative for a single-site-like catalyst structure and behavior. © 2011 Wiley Periodicals, Inc. J Appl Polym Sci 124: 4889–4896, 2012

Key words: poly(propylene-*co*-ethylene); Ziegler–Natta catalysts; NMR

INTRODUCTION

In general, poly(propylene-*co*-ethylene) random copolymers have lower melting point, crystallinity, stiffness, and better optical properties than poly(propylene) homopolymers. Typical application areas for such random copolymers are in cast and blown film and in injection molding. An important feature of films made of these copolymers is their excellent sealing properties at low temperatures. For such copolymers, a key microstructure property is randomness of ethylene units along the polymer chain. A more random ethylene distribution both lowers the melting point and crystallinity as improves the optical and sealing properties of a film. The randomness of ethylene incorporation is catalyst specific.

In propylene polymerization, hydrogen is commonly used as an effective chain transfer agent to control molecular weight. As well as being efficient at controlling molecular weight, hydrogen also has a profound effect on catalyst activity. By adding hydrogen, the activity of most Ziegler–Natta (ZN) catalysts can be increased by a factor of 3–5.

When propylene is polymerized, most monomers insert into the growing chain by regio-regular 1,2 insertions (primary insertion). A small fraction, however, of the monomers may insert by regio-irregular 2,1 insertion (secondary insertion). After such a secondary insertion, the catalytic center becomes a so-called dormant site and further polymerization is strongly inhibited until the site is released from this state.[1–4] The reactivity after a primary insertion is in the order of 100–1000 times faster than after a secondary insertion.[1,5] It was early seen that also ethylene as comonomer has an activity increasing effect in propylene polymerization with ZN polypropylene (PP) catalysts.[6,7] It has been shown that the activity increasing effect of hydrogen and ethylene is due to the ability of these species to enter the dormant sites

and release them for further polymerization. The frequency of secondary insertion has been shown, at least for some ZN PP catalysts, to correlate with hydrogen response of the catalyst. The high hydrogen response seen for a ZN catalyst with diether as an internal donor was attributed to the frequent and uniform distribution of 2,1 insertions.[5,8–12]

Although 2,1 insertions have a large influence on activity and hydrogen response during polymerization, as the likelihood of such regio errors is low for ZN catalyzed polypropylenes ($\approx$ 0.1 mol %), their presence in the final chain has little influence on the final polymer microstructure.[1,5] In contrast, stereo errors of the catalyst, and their associated stereo defects in the chain, are far more frequent and have a far greater influence on the polymer microstructure.

Due to their multisite nature, a common feature of ZN catalysts is to produce polymers where the likelihood of defects in a chain is molecular weight dependent, i.e., short chains contain far more defects than longer chains. The consequence of this behavior for copolymers is that the shorter chains have a much higher ethylene content than longer chains. As well as absolute comonomer content, the way the comonomer is distributed along the chains is very important for copolymers, specifically how randomly the ethylene units are distributed. A more random distribution of the ethylene units results in shorter isotactic propylene sequences; this in turn results in thinner lamella and thus lower melting point. To some extent, ethylene containing segments may be included in crystalline regions, but these still disturb the crystal structure and lower the melting point and crystallinity.[13–16]

In contrast, single site (SS) catalysts, by definition, only have one type of site, the consequences of which are expressed in the structures of the polymers which they produce. Ethylene propylene copolymers produced with SS catalysts has an even distribution of comonomer between short and long chain[17] and due to a more ideal random distribution of ethylene along the chains lower melting points.[18]

This article describes investigations concerning the activity of two ZN catalysts during copolymerization of propylene and ethylene at low ethylene content. In addition, a study of the structure and thermal properties of the resulting polymers was also undertaken. The first catalyst (A) was produced with the so-called Sirius technology, which gives completely compact catalyst particles without internal pore volume. Despite the compact nature of this catalyst, it has previously been shown to exhibit good powder morphology and high activity during polymerization.[19–21] The second catalyst (B) can be described as a conventional fourth generation ZN PP catalyst.

EXPERIMENTAL PROCEDURE

Materials

Propylene was obtained from a polypropylene plant (Borealis, Finland) after purification, and it was further dried with molecular sieves before use in polymerization. Pentane was dried with molecular sieves and purged with nitrogen. Triethyl aluminium (TEA) was obtained from Chemtura and was used as received. Dicyclopentyl dimethoxy silane (DCP) was obtained from Wacker and was dried with molecular sieves and purged with nitrogen before use. The hydrogen (AGA) was of 99.999% purity. Ethylene with 99.95% purity was obtained from AGA, and it was further purified with molecular sieves before use.

Catalyst

Two catalysts were used, hereafter referred to as Catalyst A and Catalyst B. Catalyst A was prepared using the Sirius technology, an emulsion-based catalyst preparation technology developed by Borealis and described elsewhere.[19] A special feature of the Sirius technology is that no separately prepared support is added during catalyst synthesis, with the $MgCl_2$ that acts as support in the final catalyst being prepared *in situ* during catalyst preparation. Catalysts prepared using this technology have no measurable pore volume and a very low surface area ($\ll$5 m^2) according to Brunauer–Emmet–Teller analysis.[21] The internal donor in Catalyst A was diethylhexyl phthalate (DOP), and the titanium content was 3.1 wt %.

Catalyst B can be described as a traditional fourth generation ZN PP catalyst with $MgCl_2$ as support. Preparation of catalyst B is described elsewhere.[22] The internal donor in catalyst B was diethyl phthalate (DEP), and the titanium content was 1.9 wt %.

Polymerization

Polymerization reactions were performed in 1400 g of liquid propylene at 70°C in a 5 L reactor with TEA as cocatalyst and DCP as external donor. The molar ratio between TEA and Ti (Al/Ti) was 250, and the molar ratio between external donor and Ti (D/Ti) was 25. The catalyst was added to the reactor via a syringe followed by hydrogen and propylene at room temperature. The temperature was increased to 70°C over a period of 16 min. The ethylene feed was controlled by a flow controller and was started after 5 min when the temperature was 40°C. After reaching 70°C, the pressure was kept constant by feeding ethylene. Two sets of polymerizations were performed. In the first set, the polymerization time was 1 h, and the amount of hydrogen was adjusted

to get molecular weight about 280,000 and 360,000 g/mol. The propylene conversion was 35%–60% in this set of experiments. In the second set, the polymerization time was 15 min and the conversion was only 1%–12%. The concentration of ethylene and hydrogen in the liquid phase in the 15-min polymerizations were calculated with Aspen Plus using the equation of state model according to Soave-Redlich-Kwong.

Analyses

The amount of xylene soluble (XS) was measured by dissolving a known amount of polypropylene in boiling xylene. After cooling to room temperature, the insoluble part was filtered off, and the solution was evaporated to dryness and weighed.

Gel permeation chromatography (GPC) was performed at 140°C using a Waters Alliance GPCV 2000 (Waters, Milford, MA). A set of three columns TSK GMHHXLHT (TosoHaas GmbH, Stuttgart, Germany) was used. The mobile phase was 1,2,4-trichlorobenzene, and the flow rate 1 mL/min was used. An injection volume of 220 μL was used at a concentration of 0.5 mg/mL. To prevent degradation 0.1 mg/mL of the stabilizer BHT was used.

Differential scanning calorimetry (DSC) was used to determine the melting temperature and was undertaken on a Mettler Toledo DSC 822[e]. The heat capacity was calibrated using water, indium, lead, zinc, and tin. After first melting, the cooling rate was set to 10°C/min as was the heating rate of the second heating. The melting point was defined as the peak of the second melting.

Quantitative $^{13}C\{^1H\}$ NMR spectra were recorded in the solution-state using a Bruker Advance III 400 NMR spectrometer operating at 400.15 and 100.62 MHz for ^1H and ^{13}C, respectively. All spectra were recorded using a ^{13}C optimized 10 mm extended temperature probehead at 125°C using nitrogen gas for all pneumatics. Approximately 200 mg of material was dissolved in 3 mL of 1,2-tetrachloroethane-d_2 (TCE-d_2) along with chromium-(III)-acetylacetonate (Cr(acac)$_3$) resulting in a 65 mM solution of relaxation agent in solvent.[23] To ensure a homogenous solution, after initial sample preparation in a heat block, the NMR tube was further heated in a rotatary oven for at least 1 h. On insertion into the magnet, the tube was spun at 10 Hz. Standard single-pulse excitation was used without NOE, using an optimized tip angle, 1 s recycle delay and a bi-level WALTZ16 decoupling scheme.[24,25] A total of 6144 (6k) transients were acquired per spectra. This setup was chosen primarily for the high resolution and quantitatively needed for accurate ethylene content quantification. Quantitative $^{13}C\{^1H\}$ NMR spectra were processed, integrated, and relevant quantitative properties determined from the integrals using custom automation programs. All chemical shifts were indirectly referenced to the central methylene group of the ethylene block (EEE) at 30.00 ppm using the chemical shift of the solvent. This approach allowed comparable referencing even when this structural unit was not present.

Characteristic signals corresponding to 2,1-erythro and 2,1-threo regio defects were not observed.[26–28]

The comonomer content was quantified using the method of Wang and Zhu[28] through integration of multiple signals across the whole spectral region in the $^{13}C\{^1H\}$ spectra. This method was chosen for its robust nature and ability to account for the presence of regio-defects when needed. Integral regions were slightly adjusted to increase applicability across the whole range of encountered comonomer contents.

The comonomer sequence distribution at the triad level was determined using the method of Kakugo et al.[29] The comonomer content [E] and comonomer distribution at the diad level was calculated from the triad distribution using known necessary relationships. The average propylene sequence length was calculated according to Randall from the triad sequence distribution using the relationship: 2[P]/[EP].[30] The amount of isolated ethylene units, which can be taken to indicate the randomness of ethylene incorporation, was calculated using the relationship: [PEP]/[E].

Infrared (IR) spectroscopy was undertaken on Nicolet Magna IR Spectrometer 550. A 220–250 μm film was prepared from the polymer powder at 230°C followed by rapid cooling to room temperature. All IR analysis was done within 2 h of film preparation. Quantitative comonomer contents were obtained using peak areas normalized to the peak height of an internal reference band calibrated to previous ^{13}C NMR results. Ethylene was quantified using the band at 733 cm^{-1} (baseline 690–780 cm^{-1}), and the reference band at 809 cm^{-1} (baseline 750–890 cm^{-1}). The amount of isolated ethylene units (randomness) was estimated using the peak height of the band at 733 cm^{-1} (baseline 690–780 cm^{-1}) and the same reference band described above. Calibration was made to previously obtained ^{13}C NMR results.

RESULTS AND DISCUSSION

The well-known effects of hydrogen and ethylene on the polymerization activity with ZN PP catalysts were observed for the two catalysts; low molecular weight homo PP was produced with higher activity than high molecular weight homo PP, due to more hydrogen being present for the low molecular weight homo PP, and the activity increased with
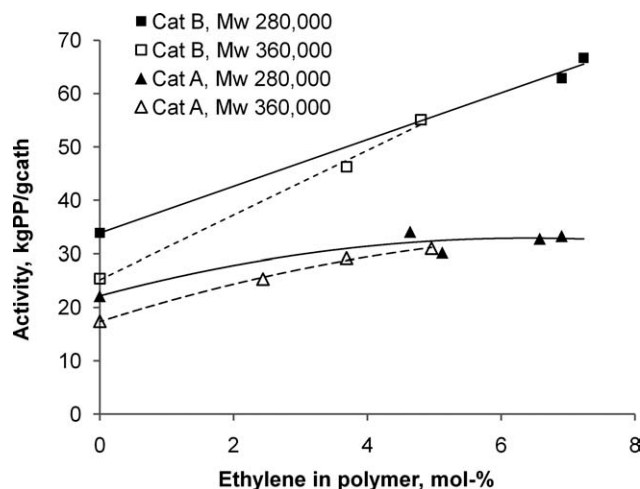
Figure 1 The influence of ethylene content (IR) on activity for different molecular weight polymers produced by catalyst A and catalyst B in 1-h polymerization.

increasing ethylene content of the polymer (Fig. 1). The difference in activity between low and high molecular weight polymers became less significant with increasing ethylene content. This observation can be explained by assuming that most of the dormant sites have been reactivated at high concentration of hydrogen and ethylene, and thus any further increase in ethylene concentration has little activity increasing effect any longer. This behavior is clearly shown for catalyst A, where a plateau value in activity was reached.

For catalyst B, ethylene increased the activity with about 100% for both low and high molecular weight systems. For catalyst A, the maximum increase in activity was only about 50%, which is clearly lower than was observed for catalyst B. In a previous study of the same catalysts, the analyses of the chain end distribution in the oligomer fraction and polymer showed that catalyst A formed about 50% more n-butyl-terminated chains than catalyst B.[31] With n-butyl end groups formed, when the growing chain is ended by chain transfer to hydrogen directly after regio irregular 2,1 insertion the higher amount of n-butyl-terminated chains indicated that catalyst A had a high degree of dormancy. In principle, the dormancy of a catalyst is dictated by the frequency of 2,1 insertions and by the time a growing chain stays in the dormant stage. It has also previously been shown that catalysts using diether as internal donor give a high concentration of n-butyl terminated oligomers,[8] indicating a high degree of dormancy, and associated polymers with a higher frequency of 2,1 insertion.[5,10,11] For this catalyst, the high concentration of n-butyl-terminated chains was at least partly due to high frequency of 2,1 insertions. On this basis, the relatively low increase in

activity with ethylene for catalyst A was surprising considering the indicated high degree of dormancy.

The observed relatively low increase in activity with ethylene could be due to differences in monomer diffusion, but no such difference has been observed between polymer particles produced with the compact catalyst A and porous catalyst B.[32]

The origin for this apparent discrepancy between the expected and observed activation behavior with ethylene content for the two catalysts can be explained when considering the activity in the 15-min polymerization (Fig. 2). In the absence of both hydrogen and ethylene, the activity of catalyst A was rather low; however, in the presence of ethylene and especially hydrogen, the activity is significantly increased, relatively seen more so than for catalyst B. The combined influence of both hydrogen and ethylene increased the activity for catalyst A by a factor of 9, whereas for catalyst B only a factor of 5 is observed. This observation is in agreement with the high degree of dormancy previously observed for catalyst A.[31] A similar trend, albeit weaker, was also observed for the 1-h polymerizations when comparing polymerization with and without both hydrogen and ethylene (Table I).

Hydrogen was more effective in increasing activity than ethylene (Fig. 2). While, ethylene roughly doubled the activity for both catalysts hydrogen increased the activity by a factor of 6 for catalyst A and 3 for catalyst B. This higher increase in activity seen for catalyst A was in line with the higher degree of dormancy observed for this catalyst.

For ZN PP catalysts, the reactivity of ethylene is typically several times higher than that of propylene, with this behavior enhanced if polymerization continues for long times (several hours). This behavior is believed to be due to a change in oxidation state
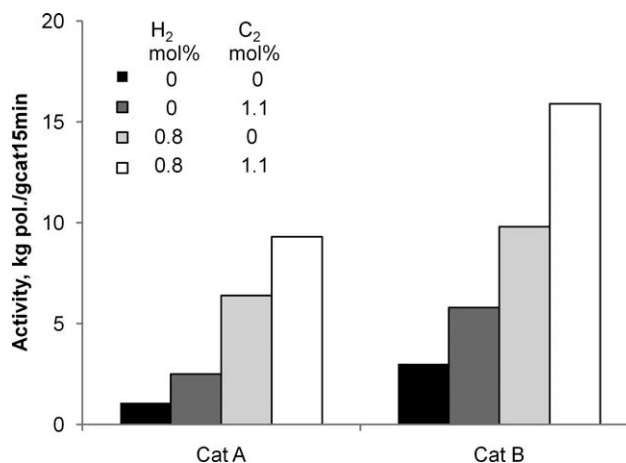

Figure 2 Comparison of activity in 15-min polymerization with and without hydrogen and/or ethylene (concentrations are those in liquid propylene phase).

TABLE I
Properties of Polymers Produced with Catalyst A and B in 1-h Polymerization with
Targeted Molecular Weights of 280,000 and 360,000 mol/g

Catalyst type	Catalyst (mg)	H_2 (mmol)	Activity (kg pol/gcath)	M_w (kg/mol)	MWD	C_2 (IR) (mol %)
A	27.4	0	4.8	–	–	0
A	34.9	90	17.4	351	4.1	0
A	24.7	112	25.3	370	3.8	2.4
A	22.2	130	29.2	352	3.6	3.7
A	19.1	145	31.0	346	3.6	5.0
A	15.5	180	22.1	280	4.1	0
A	16.1	300	33.1	275	4.0	4.6
A	15.3	300	30.2	270	4.2	5.1
A	14.0	300	32.8	267	4.2	6.6
A	14.1	300	33.3	261	3.7	6.9
B	12.8	0	10.1	–	–	0
B	10.8	110	25.4	364	4.9	0
B	14.8	200	46.3	380	4.5	3.7
B	11.2	225	55.1	352	5.0	4.8
B	8.5	220	33.9	283	5.3	0
B	7.6	370	62.9	285	5.0	6.9
B	7.5	370	66.7	292	5.0	7.2

of titanium toward Ti^{2+}, which can polymerize ethylene but is inactive toward propylene. In the 15-min polymerizations in this study, the reactivity toward ethylene was about three times higher than that of propylene (Fig. 3). Catalyst A was also shown to have a higher reactivity toward ethylene than catalyst B. It can be speculated that the higher reactivity of ethylene with catalyst A was due to the higher degree of dormancy, using a similar logic used to explain the high hydrogen response of a ZN PP catalyst with diether as internal donor.[11] However, the frequency of secondary insertions is very low ($\approx$ 0.1 mol %), whereas the ethylene content was relatively high (3–5 mol %). It must therefore be questioned if a small difference in dormancy, due to 2,1 insertions, between catalysts is significant for the reactivity toward ethylene. From previous studies of tacticity by NMR, it is known that catalyst A has a higher likelihood of making stereo errors, and thus produces more stereo defects in the chain, than catalyst B.[31] Hence, it could be speculated that the higher frequency of stereo irregular insertions seen for catalyst A improves the ethylene reactivity of the catalyst. This hypothesis thus assumes that ethylene insertion is faster after a stereo irregular insertion than after a stereo regular insertion.

After secondary insertion, hydrogen and ethylene compete for access to the active center, this is shown by the ethylene content of a polymer being about 50% higher if hydrogen is not present during polymerization (Table II). This observation supports the idea that a higher degree of dormancy leads to higher ethylene incorporation and explains the observed difference in ethylene response between the two catalysts.

The effect of ethylene, hydrogen, and degree of dormancy, due to 2,1 insertions, on activity and ethylene incorporation for these two catalysts is much in line with earlier results with ZN catalyzed copolymerization of propylene and ethylene reported in literature. More important is the effect of the emulsion-based Sirius catalyst preparation technology on polymer structure.

The microstructure of the produced copolymers was analyzed by ^{13}C-NMR spectroscopy. To emphasize the different incorporation behavior of the two catalysts, two copolymers with approximately the same ethylene content was compared.

For the copolymer produced by catalyst A, ethylene was found to be more evenly distributed between the xylene soluble and insoluble fractions,
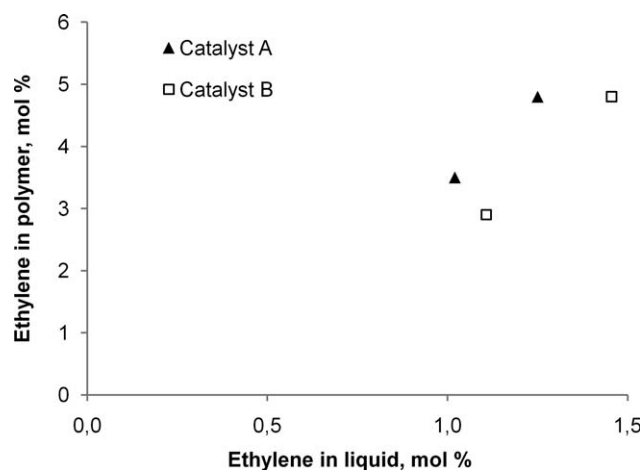
Figure 3 The correlation of ethylene incorporation in the polymer (IR) with ethylene concentration in the liquid propylene phase in 15-min polymerizations.

TABLE II
Activity in 15-min Polymerization and Properties of the Polymers Produced. The catalyst amount was 10–15 mg

Catalyst type	Polymerization				Polymer				
	H_2^a (mmol)	C_2^b ΔP (bar)	C_2^c (mol %)	Activity (kg pol/ gcat15 min)	C_2^d (IR) (mol %)	R^e (IR) (%)	T_m (°C)	M_w (kg/mol)	MWD
A	0	0	0	1.07	0	–	163.6	–	–
A	400	0	0	6.4	0	–	163.4	186	7.1
A	0	0.77	1.2	2.5	5.4	71.9	144.7	–	–
A	400	0.69	1.0	9.3	3.5	83.3	148.2	203	6.1
A	400	0.85	1.3	8.5	4.8	78.3	144.7	210	5.5
B	0	0	0	3.0	0	–	166.0	–	–
B	400	0	0	9.8	0	–	164.5	227	7.2
B	0	0.85	1.3	5.8	4.5	68.0	150.1	–	–
B	400	0.75	1.1	15.9	2.9	80.8	153.9	240	7.0
B	400	0.96	1.5	16.0	4.8	70.7	150.0	250	7.5

[a] 400 mmol hydrogen corresponds to 0.8 mol % in the liquid propylene phase as calculated with Aspen.
[b] Partial pressure of ethylene in the reactor.
[c] Ethylene concentration in the liquid propylene phase as calculated with Aspen.
[d] Ethylene content in the polymer as determined by IR.
[e] The amount of isolated ethylene units (randomness) as determined by IR.

when compared with the copolymer produced by catalyst B (Table III). Although the xylene insoluble fractions had roughly the same ethylene content ~ 4 mol %, the soluble fractions for catalyst A and B contained 19 and 29 mol % of ethylene, respectively. This is an indication that ethylene distribution between long and short chains is more even for catalyst A than for catalyst B.

With respect to the distribution of the ethylene units along the chain, the comonomer sequence distribution at the triad level determined from NMR provides clear differences between catalysts. From the xylene insoluble fraction, it is clearly seen that the tendency to form ethylene triads (EEE) was significantly lower for catalyst A than catalyst B. Similarly, the occurrence of isolated ethylene units (represented by PEP) was significantly higher for catalyst A than for catalyst B. Both these observations indicate that ethylene was more randomly distributed with catalyst A. As well as the comonomer sequence distribution itself, the statistical properties derived from it also indicate more random behavior for catalyst A. For example, the shorter average propylene sequence length also suggests a more random distribution of ethylene for catalyst A. Both the ethylene distribution between the xylene soluble and

TABLE III
Microstructure of Copolymers Produced by Both Catalysts in 15 minute Polymerizations and Their Respective Xylene Insoluble and Xylene Soluble Fractions as Determined by ^{13}C NMR

Catalyst Polymer fraction		A Whole sample	B Whole sample	A Xylene insoluble	B Xylene insoluble	A Xylene soluble	B Xylene soluble
Weight fraction	(wt %)	100	100	93.4	92.6	6.6	7.4
C2^a	(mol %)	4.7	5.3	4.1	4.0	18.8	29.4
E^b	(mol %)	5.2	5.1	4.2	3.8	18.2	28.5
EEE	(mol %)	0.1	0.5	0.0	0.2	2.0	6.2
EEP	(mol %)	1.2	1.3	0.7	0.4	5.6	10.5
PEP	(mol %)	3.9	3.3	3.5	3.2	10.6	11.8
EPE	(mol %)	0.4	0.5	0.1	0.1	3.3	6.8
EPP	(mol %)	8.0	7.0	7.3	6.4	21.4	21.3
PPP	(mol %)	86.5	87.4	88.3	89.9	57.2	43.4
C3 sequence length^c	n	22	24	25	29	6	4
Randomness^d	(%)	81	62	86	80	56	40

[a] Ethylene content of copolymer determined according to Wang et al.[28]
[b] Ethylene content of copolymer determined from triads, i.e., [EEE]+1/2[EEP]+[PEP].
[c] Average sequence length determined as 2[P]/[EP].
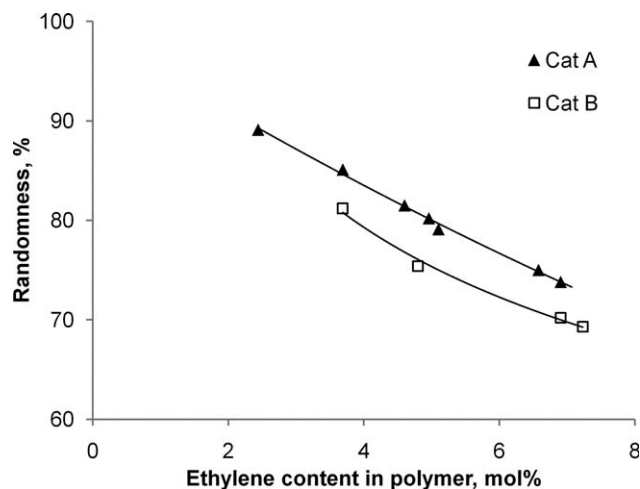[d] The amount of isolated ethylene units (randomness) determined as [PEP]/[E].

Figure 4 The correlation of randomness by IR with ethylene content for polymers produced in 1-h polymerization.

Figure 5 The correlation of melting point with ethylene content (from IR) for polymers produced in 1-h polymerization.

insoluble fractions and the more random ethylene incorporation suggest that catalyst A had a more narrow distribution of active site types than catalyst B.

A similar trend with respect to how random the ethylene was incorporated for the two catalysts was also observed by IR spectroscopy (Fig. 4), supporting the NMR derived properties. Catalyst A gave about 5% higher randomness than catalyst B at a given ethylene content.

The implication of a more random incorporation of comonomer was clearly expressed through the thermal properties (Fig. 5). For copolymers produced with catalyst A, about a 5°C lower melting point was observed, when compared with those produced with catalyst B at high ethylene content.

The amount of XS also indicates differences between the catalysts. At medium ethylene content, the XS was lower for catalyst A, but at higher ethylene contents, the trend was reversed (Fig. 6). The effect of ethylene on the amount of XS is much smaller for SS catalysts than for ZN PP catalysts.[33–35] With SS catalysts, XS increases only marginally with increasing ethylene content up to a point above which XS increases very rapidly. The behavior of catalyst A goes slightly into the same direction (Fig. 6).

From this study (Tables I and II) and previous work,[31] it can be seen that catalyst A gave narrower molecular weight distribution (MWD) than catalyst B. With the other structural differences between polymers produced with catalyst A and catalyst B reported here, this showed that catalyst A has a narrower active site type distribution than catalyst B. As different internal donors (DOP or DEP) and catalyst technology (Sirius or traditional) were used, in principal it is not possible to conclude which contributes more to the narrow distribution of active
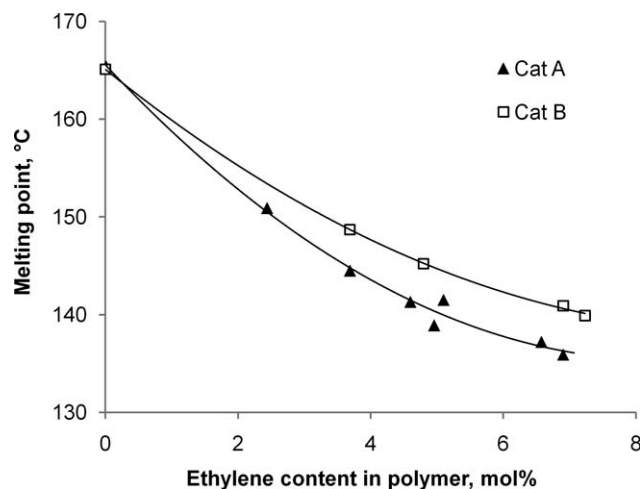
site types for catalyst A. It is known that the internal donor influences on the formation of the $MgCl_2$-crystallite lateral edges. Ethyl benzoate and di-isobutyl phthalate, as internal donors, give slightly different setup of $MgCl_2$ crystal forms and via this possibly also different active center types.[36] However, it is believed that the formation of active sites under the more defined homogeneous conditions, typical for emulsion-based Sirius technology, is the main reason for the narrower active site type distribution. The considerable effect of this catalyst preparation method on the formation of active sites can also be seen in the rather unique magnesium dichloride structure of the catalyst particles. Powder XRD measurements revealed the presence of δ-magnesium dichloride in form of a chain-like structure. The chains extended from the center of the catalyst particle to the surface, and the internal donor and
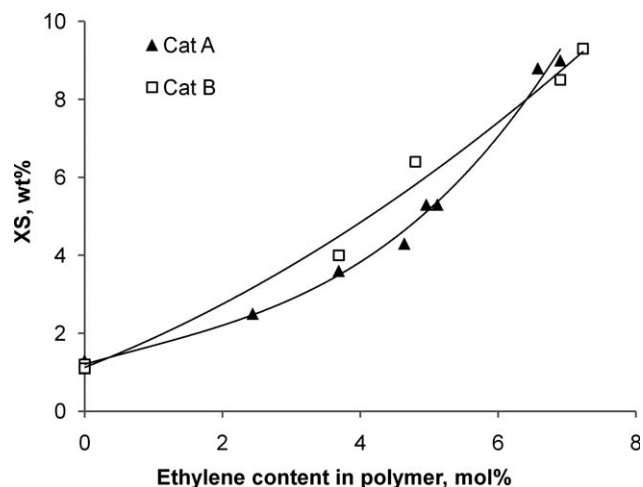

Figure 6 The correlation of XS with ethylene content (from IR) for polymers produced in 1-h polymerization.

the polymerization active titanium centers coordinated to these magnesium dichloride nanoribbons. Thereby, a porous structure was created, where the titanium was homogeneously distributed within the entire catalyst particles.[37]

Comparison of the powder XRD diffractogram of catalyst A[37] and catalyst B[22] shows that the peak in the 10°–20° area is located at slightly higher 2θ values for catalyst A than for catalyst B. The peak is located at 14°–19° with the highest value at 16.3° for catalyst A. The corresponding values for catalyst B is 11°–18° with the highest value at 14°–15°. This peak is related to the stacking of Cl-Mg-Cl triple layers along the crystallographic direction and the slightly higher 2θ value for catalyst A indicates that the interlayer distance is shorter for this catalyst. This can be due to less distortion in the $MgCl_2$ structure giving a more regular arrangement of the Cl-Mg-Cl triple layers, which in turn can be attributed to the homogeneous catalyst preparation conditions. A more regular Cl-Mg-Cl triple layer structure can be one reason to the observed narrow active site type distribution with catalyst A.

In general, it has been shown that even if catalyst A is a ZN PP catalyst, it does have some key features which differentiate it from a typical multisite ZN PP catalyst, importantly these features tend to a certain degree to be more indicative for single-site-like catalyst behavior.

CONCLUSIONS

In conclusion, it was shown that ethylene was more readily incorporated with catalyst A than catalyst B and that the nature of the active sites is not exactly the same for the two different catalyst preparation procedures and thereby resulting in variation of average polymer properties. Moreover, the combined effect of hydrogen and ethylene on activity was greater for catalyst A, which is believed to be due to the higher degree of dormancy, due to 2,1 insertions, with this catalyst. From polymer microstructure analysis by NMR and IR, a more random incorporation of ethylene was found for catalyst A and confirmed by thermal analysis. In addition to comonomer incorporation, catalyst A also gave a narrower MWD. All observations suggest that catalyst A has a narrower distribution of active site types, which is believed to originate from the emulsion-based Sirius catalyst preparation technology.

References

1. Busico, V.; Cipullo, R.; Corradini, P. Makromol Chem 1993, 194, 1079.
2. Busico, V.; Cipullo, R.; Corradini, P. Makromol Chem Rapid Commun 1993, 14, 97.
3. Tsutsui, T.; Kashiva, N.; Mizonu, A. Macromol Chem Rapid Commun 1990, 11, 565.
4. Busico, V.; Cipullo, R.; Chadwick, J. C.; Modder, J. F.; Sudmeijer, O. Macromolecules 1994, 27, 7538.
5. Busico, V.; Cipullo, R.; Polzone, C.; Talarico, G.; Chadwick, J. C. Macromolecules 2003, 36, 2616.
6. Spitz, R.; Masson, P.; Bobichon, C.; Guyot, A. Makromol Chem 1988, 189, 1043.
7. Spitz, R.; Masson, P.; Bobichon, C.; Guyot, A. Makromol Chem 1989, 190, 717.
8. Chadwick, J. C.; Morini, G.; Balbontin, G.; Camurati, I.; Heere, J. J. R.; Mingozzi, I.; Testoni, F. Macromol Chem Phys 2001, 202, 1995.
9. Chadwick, J. C.; Morini, G.; Albizzati, E.; Balbontin, G.; Mingozzi, I.; Cristofori, A.; Sudmeijer, O.; Van Kessel, G. M. M. Macromol Chem Phys 1996, 197, 2501.
10. Busico, V.; Cipullo, R.; Ronca, S. Macromolecules 2002, 35, 1537.
11. Busico, V.; Chadwick, J. C.; Cipullo, R.; Ronca, S.; Talarico, G. Macromolecules 2004, 37, 7437.
12. Chadwick, J. C.; Van der Burgt, F. P. T. J.; Rastogi, S.; Busico, V.; Cipullo, R.; Talarico, G.; Heere, J. J. R. Macromolecules 2004, 37, 9722.
13. De Rosa, C.; Auriemma, F.; de Ballesteros, O. R.; Resconi, L.; Camurati, I. Chem Mater 2007, 19, 5122.
14. Hosoda, S.; Hori, H.; Yada, K.; Nakahara, S.; Tsuji, M. Polymer 2002, 43, 7451.
15. Gou, Q.; Li, H.; Yu, Z.; Chen, E.; Zhang, Y.; Yan, S. Chin Sci Bull 2008, 53, 1804.
16. Hosier, I. L.; Alamo, R. G.; Lin, J. S. Polymer 2004, 45, 3441.
17. Suárez, I.; Caballero, M. J.; Coto, B. Eur Polym J 2010, 46, 42.
18. Fujiyama, M.; Inata, H. J Appl Polym Sci 2002, 85, 1851.
19. Abboud, M.; Denifl, P.; Reichert, K. H. J Appl Polym Sci 2005, 98, 2191.
20. Abboud, M.; Denifl, P.; Reichert, K. H. Macromol Mater Eng 2005, 290, 1220.
21. Vestberg, T.; Denifl, P.; Wilen, C. E. J Appl Polym Sci 2008, 110, 2021.
22. Garoff, T.; Leinonen, T.; Iiskola, E. Patent WO9219658 1992.
23. Singh, G.; Kothari, A.; Gupta, V. Polym Test 2009, 28, 475.
24. Zhou, Z.; Kuemmerle, R.; Qiu, X.; Redwine, D.; Cong, R.; Taha, A.; Baugh, D.; Winniford, B. J Magn Reson 2007, 187, 225.
25. Busico, V.; Carbonniere, P.; Cipullo, R.; Pellecchia, R.; Severn, J.; Talarico, G. Macromol Rapid Commun 2007, 28, 1128.
26. Resconi, L.; Cavallo, L.; Fait, A.; Piemontesi, F. Chem Rev 2000, 100, 1253.
27. Cheng, H. N. Macromolecules 1984, 17, 1950.
28. Wang, W. J.; Zhu, S. Macromolecules 2000, 33, 1157.
29. Kakugo, M.; Naito, Y.; Mizunuma, K.; Miyatake, T. Macromolecules 1982, 15, 1150.
30. Randall, J. Macromol Sci Rev Macromol Chem Phys 1989, C29, 201.
31. Vestberg, T.; Denifl, P.; Parkinson, M.; Wilén, C. E. J Polym Sci Part A: Polym Chem 2010, 48, 351.
32. Bartke, M.; Oksman, M.; Mustonen, M.; Denifl, P. Macromol Mater Eng 2005, 209, 250.
33. Bidell, W.; Fischer, D.; Grasmeder, J.; Gregorius, H.; Hingmann, R.; Jones, P.; Langh, F. Metcon, June 4–5, 1997, Houston, Texas.
34. Hungenberg, K. D.; Kerth, J.; Langhauser, F.; Müller, H. J.; Müller, P. Angew Makromol Chem 1995, 227, 159.
35. Schulte, J.; Sell, T.; Grant, T. M.; Winter, A.; Dimeska, A. Patent WO2009054831 2009.
36. Singh, G.; Kaur, S.; Makawana, U.; Patankar, R. B.; Gupta, V. K. Macromol Chem Phys 2009, 210, 69.
37. Rönkkö, H. L.; Knuuttila, H.; Denifl, P.; Leinonen, T.; Venäläinen, T. J Mol Catal A: Chem 2007, 278, 127.